frontiers in Built Environment

ORIGINAL RESEARCH
published: 13 June 2017
doi: 10.3389/fbuil.2017.00033

Engineering Properties of Treated Natural Hemp Fiber-Reinforced Concrete

Xiangming Zhou, Harmeet Saini and Gediminas Kastiukas*

Division of Civil Engineering, Department of Mechanical, Aerospace and Civil Engineering, Brunel University London, Uxbridge, United Kingdom

In recent years, the construction industry has seen a significant rise in the use of natural fibers, for producing building materials. Research has shown that treated hemp fiber-reinforced concrete (THFRC) can provide a low-cost building material for residential and low-rise buildings, while achieving sustainable construction and meeting future environmental targets. This study involved enhancing the mechanical properties of hemp fiber-reinforced concrete through the $Ca(OH)_2$ solution pretreatment of fibers. Both untreated (UHFRC) and treated (THFRC) hemp fiber-reinforced concrete were tested containing 15-mm length fiber, at a volume fraction of 1%. From the mechanical strength tests, it was observed that the 28-day tensile and compressive strength of THFRC was 16.9 and 10% higher, respectively, than UHFRC. Based on the critical stress intensity factor (K^s_{IC}) and critical strain energy release rate (G^s_{IC}), the fracture toughness of THFRC at 28 days was also found to be 7–13% higher than UHFRC. Additionally, based on the determined brittleness number (Q) and modulus of elasticity, the THFRC was found to be 11% less brittle and 10.8% more ductile. Furthermore, qualitative analysis supported many of the mechanical strength findings through favorable surface roughness observed on treated fibers and resistance to fiber pull-out.

Keywords: fiber treatment, fracture, FRC, hemp fiber, natural fiber-reinforced concrete

OPEN ACCESS

Edited by:
Huisu Chen,
Southeast University, China

Reviewed by:
M. Iqbal Khan,
King Saud University, Saudi Arabia
Sriramya Duddukuri Nair,
University of Texas at Austin, United States
Wang Qiang,
Tsinghua University, China

****Correspondence:***
Xiangming Zhou
xiangming.zhou@brunel.ac.uk

Specialty section:
This article was submitted to Structural Materials, a section of the journal Frontiers in Built Environment

Received: *23 March 2017*
Accepted: *16 May 2017*
Published: *13 June 2017*

Citation:
Zhou X, Saini H and Kastiukas G (2017) Engineering Properties of Treated Natural Hemp Fiber-Reinforced Concrete. Front. Built Environ. 3:33. doi: 10.3389/fbuil.2017.00033

INTRODUCTION

In recent years, the construction industry has been driven to make some changes with respect to sustainability. The latest government regulations are prescribing that by the year 2020, all new buildings will need to have an emissions footprint close to 0 (Concerted Action Energy Performance of Buildings, 2010) and actively contribute to the decarbonization target of 80% by the year 2050 (GOV, 2011). Buildings will need to become better insulated, obtain their heating from low-carbon sources, and be built from sustainably sourced raw materials.

Concrete is one of the most widely used building materials in the world due to its abundance, affordability, and unique properties that make it so durable. However, concrete is a brittle material that exhibits low tensile strength, strain capacity, fracture toughness, and poor energy absorption. The latter disadvantages can be mitigated through reinforcement using either steel or synthetic fibers manufactured from polypropylene nylon or polyvinyl alcohol. The use of steel or synthetic fibers is expensive and damaging to the environment from a production point of view.

The use of natural fiber reinforcement, on the other hand, can be traced back almost 5,000 years; asbestos fibers were used to reinforce clay pots in Scandinavia (Bledzki et al., 2002), and similarly, the Egyptians used straw fibers to reinforce mud blocks for building walls (Mehta and Monteiro, 2006).

The main markets for natural fibers that still remain are predominantly based on developing countries where they are locally available and cheap to acquire. However, the use of natural fibers in developed countries is still limited, as it has not been fully accepted as an alternative to synthetic fibers. The long-term durability of natural fiber-reinforced concrete (NFRC) is limited due to their high permeability and lack of resistance to crack growth, particularly fibers obtained from agricultural by-products (Stevulova et al., 2014). A major problem of natural plant fibers compared to synthetic fibers is the lack of material homogeneity and hydrophility of natural fibers resulting in high moisture absorption.

Unlike manufactured fibers, natural lignocellulosic fibers contribute to a more sustainable building resource. The environmental impact of natural fibers is minuscule compared to manufactured fibers, as they can be locally grown and require a low amount of energy for processing. This reduces the CO_2 emissions associated with transportation and manufacturing, hence, achieving a lower embodied energy value. In fact, natural fibers have been assessed to be carbon negative when the whole life cycle is considered, as plants absorb carbon dioxide and release oxygen into the air as part of the natural photosynthesis process.

Research has demonstrated that adding natural fibers to concrete can, in fact, enhance its engineering properties. For example, the fracture toughness, tensile strength, flexural strength, fatigue, and impact resistance are all seen to be improved (Mehta and Monteiro, 2006). Additionally, adding fibers to a concrete matrix has been long recognized as a way to enhance the energy absorption capacity and crack resistance of regular concrete (Merta and Tschegg, 2013). Natural fibers have also been reported to improve concrete insulation properties by a reduction in its thermal conductivity by 25–35% (Awwad et al., 2012), enabling for a potential reduction in a building's heat consumption.

Nonetheless, the inclusion of untreated natural fibers has been reported to deliver reduced compressive strength due to poor adhesion and thus bonding between the fibers and concrete matrix (Bentur and Mindess, 2007). Thus, the objective of this study is to use pretreated natural hemp fibers for concrete reinforcement, address these current issues faced, and build further on the mechanical properties of UHFRC to promote the use of natural fibers in the construction industry.

Hemp fibers are obtained from the bast of the *Cannabis sativa* L. plant and belong to the cannabis family. Hemp usually grows relatively easily with minimal upkeep and without the use of artificial fertilizers. It is able to cover a planted area within 4 weeks (Rijswijk et al., 2003), making its cultivation cheaper than other natural fibers. Processing of the hemp plant into fiber requires a series of processes involving removal of the seeds, retting, drying, and, sorting to be left with evenly divided bunches of hemp strands. The fiber strands are cylindrical and vary in diameter/length, often possessing irregular surfaces.

Bast fiber (the inner bark) is often seen to be a waste product and usually ends up in land fill (Morgan, 2014). This not only makes the fibers required for HFRC extremely cheap but very easily available. Another significant benefit is that the carbon trapped inside the hemp offsets the carbon from the hemp production and also the residual carbon from the lime production after reabsorption as the lime cures (Ray, 2015).

MATERIALS AND METHODS

Materials

A concrete with a water–cement ratio (W/C) of 0.67 was prepared using a CEM II/B-V 32.5 N Portland-fly ash cement (CEMEX, UK). Shingle with a maximum particle size of 10 mm and sharp sand with a maximum particle size of 2 mm were used as the coarse and fine aggregate, respectively, in saturated surface dry conditions. The hemp fiber (shown in **Figure 1**) was acquired from Wild Fibers Ltd. (UK) in the form of 1.2-m length strands weighing 250 g. The hemp fibers were 100% natural, with no pretreatment or additional waxes applied. The hemp strands were bunched in 25 g bundles and cut to a mean length of 15 mm. Treated and untreated hemp fibers were added to concrete as 1% by volume. A density of 1,300 kg/m^3 for the untreated hemp fiber was used for the purpose of mix proportions. The complete mix design is presented in **Table 1**.

Hemp Fiber Treatment

One hundred-gram batches of 15-mm length chopped hemp fibers were submerged in 3 l solutions containing 2 wt.% $Ca(OH)_2$, as shown in **Figure 2A**. The latter solution concentration was used since it provided a satisfactory estimation of the pore water alkalinity of a fully hydrated cement paste. The hemp fibers were

FIGURE 1 | Fifteen-millimeter length hemp fibers.

TABLE 1 | Concrete mix proportions by wt.%.

W/C	Cement	Fine aggregate	Coarse aggregate
0.67	1	1.5	2.5

FIGURE 2 | Hemp fibers **(A)** submerged in $Ca(OH)_2$ solution and **(B)** drying after $Ca(OH)_2$ solution treatment.

then left to soak in the alkaline solution for 14 h, at a controlled temperature of 20°C. After soaking, the hemp fibers were drained and rinsed thoroughly with potable water to remove any excess $Ca(OH)_2$ and obtain a neutral pH. The fibers were then left again to drain for 30 min to get rid of any excess water that remained. The hemp fibers were subsequently spread out on absorbent cotton sheets in loose bunches as shown in **Figure 2B** for drying at 20°C for 48 h. This ensured even drying, reduced the effect of clumping, and when dry allowed for easy separation without damage.

Compressive and Tensile Strength Test

The compressive and tensile strength of concrete was tested according to BS EN 12390-3-2009 (British Standards Institute, 2009a) using a concrete crushing device (VJ Tech, UK). For both the compression test and tensile strength tests, cylinders with a diameter of 100 mm and a height of 200 mm were tested at 7, 14, and 28 days. For the splitting tensile strength test, a splitting tensile test device was used in accordance to EN 12390-6 (British Standards Institute, 2009b). The tensile splitting methodology was used as a simple alternative to the more complex direct tensile testing approach. In order to obtain a close estimate of the true tensile strength of FRC, the tensile strength was calculated using the load at the linear elastic limit state, as recommended by Denneman et al. (2011). A total of 36 specimens were tested, i.e., 3 specimens for each of the days mentioned, for both treated hemp fiber-reinforced concrete (THFRC) and UHFRC; the deviation of results fluctuated between 0.023 and 0.577.

Scanning Electron Microscope (SEM) Analysis

Electron microscopy was performed using the secondary electron mode (Zeiss Supra 35VP) to characterize the hemp fiber surface structure and fiber condition after HFRC fracture. Samples of HFRC were dried under vacuum and coated with a thin layer of gold layer before observation to eliminate effects of charging during image collection.

Fracture Toughness Test

The fracture toughness of concrete was determined in accordance with RILEM (TC 50-FMC and TC 89-FMT) (RILEM Draft Recommendations TC 50-FMC, 1985; RILEM Draft Recommendations TC 89-FMT, 1990) using the two parameter fracture model (TPFM) proposed by Jenq and Shah (1985) to interpret the results. The 100 mm × 100 mm × 500 mm beams were used to perform the three point bending test, which contained a notch at the mid span (the notch had a depth of 28.5 mm, a thickness of 6 mm, and a length 100 mm). For this test, an Instron 5584 K4212 hydraulic machine was used.

In accordance with the TPFM, the following equations were used with the addition of Eqs 3 and 4 (Jenq and Shah, 1985; Xu and Reinhardt, 1998, 2000):

$$Q = \left(\frac{E \times \mathrm{CTOD_c}}{K_{\mathrm{IC}}^{\mathrm{s}}}\right)^2 \tag{1}$$

$$K_{\mathrm{IC}}^{\mathrm{s}} = \frac{3\left(P_{\max} + \frac{0.5WS}{L}\right)S}{2DB^2}\sqrt{\pi a_e}\,F(a) \tag{2}$$

$$\mathrm{CTOD_c} = \frac{6\left(P_{\max} + \frac{0.5WS}{L}\right)Sa_e}{D^2BE}V_1(a)\Big\{(1-\beta)^2 + (-1.149a + 1.081)\left(\beta - \beta^{0.5}\right)\Big\}^{0.5} \tag{3}$$

$$E = \frac{6Sa_0V_1(a)}{C_iD^2B} \tag{4}$$

$$F(a) = \frac{\left[1.99 - a(1-a)\left(2.15 - 3.93a + 2.7a^2\right)\right]}{\left[\sqrt{\pi}\,(1+2a)\,(1-a)^{1.5}\right]} \tag{5}$$

$$V_1(a) = 0.76 - 2.28a + 3.87a^2 - 2.04a^3 + \frac{0.66}{(1-a)^2} \tag{6}$$

$$G_{\mathrm{IC}}^{\mathrm{s}} = \frac{\left(K_{\mathrm{IC}}^{\mathrm{s}}\right)^2}{E} \tag{7}$$

$$a = \frac{a_e}{D} \tag{8}$$

$$\beta = \frac{a_0}{a_e} \tag{9}$$

$$a_e = \frac{2}{\pi}(D+H_0)\tan^{-1}\sqrt{\frac{B \times E \times \mathrm{CMOD}}{32.6P_{\max}} - 0.1135 - H_0} \tag{10}$$

$$a = \frac{a_0 + H_0}{D + H_0} \tag{11}$$

where $\mathrm{CTOD_c}$, critical tip opening displacement; CMOD, crack mouth opening displacement; C_i, initial flexibility; C_u, unloading flexibility; $K_{\mathrm{IC}}^{\mathrm{s}}$, critical stress intensity factor; $G_{\mathrm{IC}}^{\mathrm{s}}$, critical strain energy release rate; S, span length; D, depth; B, width; L, length; E, modulus of elasticity; a_0, depth of the notch; $P_{\max}$, ultimate load; a_e, critical effective crack length; $F(\alpha)$, shape function about α; $V_1(\alpha)$, shape function about α; W, self-weight of beam; H_0, thickness of knife edge where gage is placed.

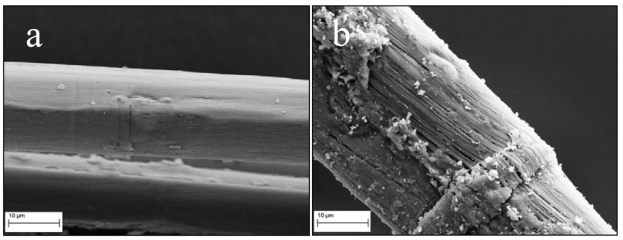

FIGURE 3 | **(A)** Untreated hemp fibers magnified at ×5,000; **(B)** $Ca(OH)_2$ solution treated hemp fibers magnified at ×5,000.

RESULTS

The surface analysis of treated and untreated hemp fibers prior to HFRC specimen production is shown in **Figure 3**. The surface of the untreated fibers shown in **Figure 3A** is observed to be smooth and non-porous, displaying parallel streaks along the length of the fiber. The surface of the fibers treated using $Ca(OH)_2$ solution is observed to be more rough and shows evidence of the expansion of the parallel streaks along the length of the fiber, which appears to penetrate deep into the interior (**Figure 3B**). In addition, the treated fiber surface contains a significant amount of debris, which indicates that even after thorough washing, the calcium hydroxide particles deposited on the fiber surface still remain. **Figure 3B** depicts that pectin in the fibers can have the ability to trap calcium as found by Sedan et al. (2007). This suggests that calcium hydroxide treatment significantly modifies the hemp fiber surface structure and increases the surface roughness. This potentially means the fibers can bond with the cement matrix more efficiently to enhance the bond strength and help to create better anchoring in the cement matrix (Mwaikambo and Ansell, 2006).

Splitting Tensile Strength

Figure 4 shows the tensile strength of THFRC and UHFRC at 7, 14, and 28 days. Initially, at 7 days, the UHFRC is shown to possess a 21% higher tensile strength. With increased curing time, the THFRC surpasses UHFRC with a 21.7 and 16.8% increase in tensile strength at 14 and 28 days, respectively. The initial disruption in the tensile strength trend at 7 days may be caused by the initial lack of a pozzolanic reaction since it is reported that pozzolanic reaction products of fly ash and calcium hydroxide take 3–14 days to initiate (Chandra and Berntsson, 1997). This would help explain why initially the tensile strength of THFRC is lower than that of UHFRC, as there is a higher $Ca(OH)_2$ content in THFRC due to the remnants of treatment residue on the fiber surface. At the early ages of around 7 days, the delayed reaction means $Ca(OH)_2$ has not yet been fully consumed for the production of calcium silicate hydrate (CSH); hence, the bond between the fiber and matrix is poor. In comparison, UHFRC bonds more sufficiently at the early ages due to the absence of $Ca(OH)_2$ on the fibers. After the 7-day interval, $Ca(OH)_2$ on the treated fibers begins to decease as a result of the peak in pozzolanic reaction, meaning more sufficient bonding and a substantially higher tensile strength at 14 days and beyond, as shown in **Figure 4**. However, the untreated fibers do not benefit from the increased formation of CSH as the pozzolanic fly ash has minimal amount

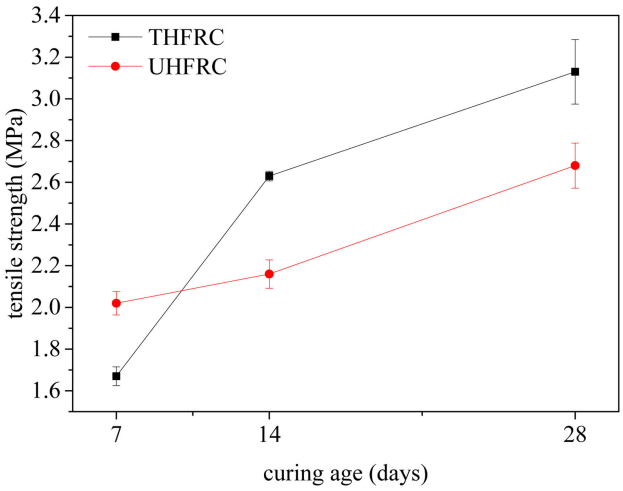

FIGURE 4 | Average tensile strength of specimens tested.

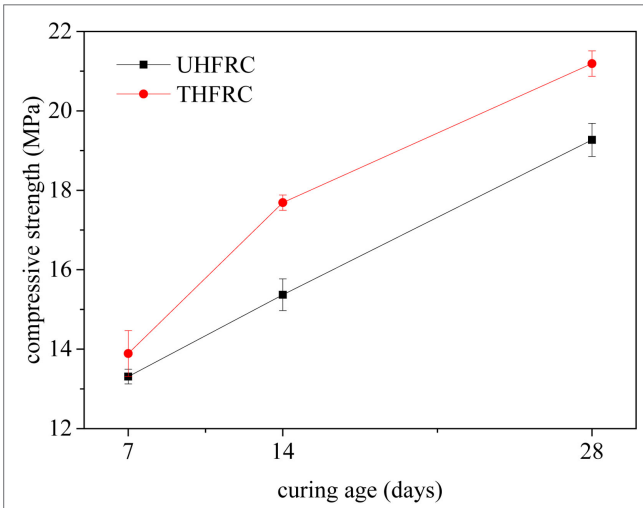

FIGURE 5 | Average compressive strength of specimens tested.

of $Ca(OH)_2$ to react with, meaning any imperfections such as micro-cracks or voids surrounding the fibers cannot be filled with CSH (Liu et al., 2014). The other reason for the observed increase in tensile strength is the enhanced fiber surface roughness resulting from the chemical treatment process; this allows for the development of an enhanced fiber–matrix bond, allowing for increased anchoring and enhanced bond strength (Mwaikambo and Ansell, 2006).

Compressive Strength

Figure 5 shows the compressive strength results of THFRC and UHFRC at 7, 14, and 28 days. The THFRC obtained compressive strengths that were 5, 15, and 10% higher than the UHFRC at 7, 14, and 28 days, respectively. This demonstrates that the inclusion of treated fibers has a positive impact on the compressive strength across all ages tested. The compressive strength of the THFRC was not observed to fall below that of UHFRC as in the case

of the tensile strength which is an indication that the higher $Ca(OH)_2$ content at 7 days has less of an effect on the compressive strength than it does on the tensile strength. This is likely to be because in compression the fibers are not directly being pulled apart as they are in tension, and therefore, the fiber–matrix bond is less significant, although still important. The higher compressive strength of THFRC at all ages can be explained by the pozzolanic reaction once again. The pozzolanic fly ash reacts with the $Ca(OH)_2$ around the treated fibers forming CSH (Rosenberg, 2010). CSH is the main product that gives concrete its strength; it is present in both the THFRC and UHFRC as a result of the reaction of Portland cement with water (Thomas, 2007). However, the additional CSH formed around the treated fibers (as shown later, in **Figure 8B**) is potentially what provides the THFRC the additional compressive strength at all ages.

Fracture Toughness

Typically in a load vs. mouth opening displacement (CMOD) curve, it can be observed that load sustained by a notched beam increases linearly until a peak is reached; once reached, the load sustained decreases non-linearly and eventually stabilizes at certain level. While this is happening, the crack continues to increase. The shape of the curve provides a good indication of the behavior of NFRC after the peak load is reached, with the fibers allowing the concrete component to stay intact for a large CMOD. Unloading tends to occur more slowly as a result of fiber bridging, providing enhanced ductility and crack resistance (Merta and Tschegg, 2013). In comparison, the unloading of plain concrete would end more abruptly at a smaller CMOD due to its brittle nature. Additionally, the length of hemp fibers plays an important role in dictating the maximum load sustained. If the length used is greater than the critical length then the ultimate strength of the fibers is achieved, whereas if the length used is smaller than the critical length then the ultimate strength of the matrix is achieved (Holister and Thomas, 1966).

From the results of the TPFM test of UHFRC and THFRC presented in **Table 2**, it can be seen that THRFC sustains 7–13% higher loads at failure, with flexural strength values of 2,158 N at 14 days and 2,488 N at 28 days. The highest peak loads at 28 days for both the UHFRC and THFRC can be simply explained by the more mature hydration stage that naturally translates as an increase in strength. **Figure 6** shows the flexural load vs. CMOD

TABLE 2 | Results for two parameter fracture test of UHFRC and treated hemp fiber-reinforced concrete (THFRC).

	Age (days)	P_{max} (N)	C_i (mm/N) $\times 10^{-6}$	C_u (mm/N) $\times 10^{-5}$	K^s_{IC} (MPa-mm$^{0.5}$)	CTOD$_c$ (mm)	G^s_{IC} (N/mm)	a_e (mm)	Q (mm)	E (MPa)
UHFRC	14	1,907	6.58	1.12	15.14	0.00789	0.0130	39.22	84.10	17,584
	28	2,325	5.65	1.13	19.97	0.00962	0.0195	42.21	97.40	20,481
THFRC	14	2,158	6.80	1.21	17.46	0.00962	0.0179	40.00	88.00	17,015
	28	2,488	6.32	1.56	23.91	0.01360	0.0313	46.08	108.10	18,279

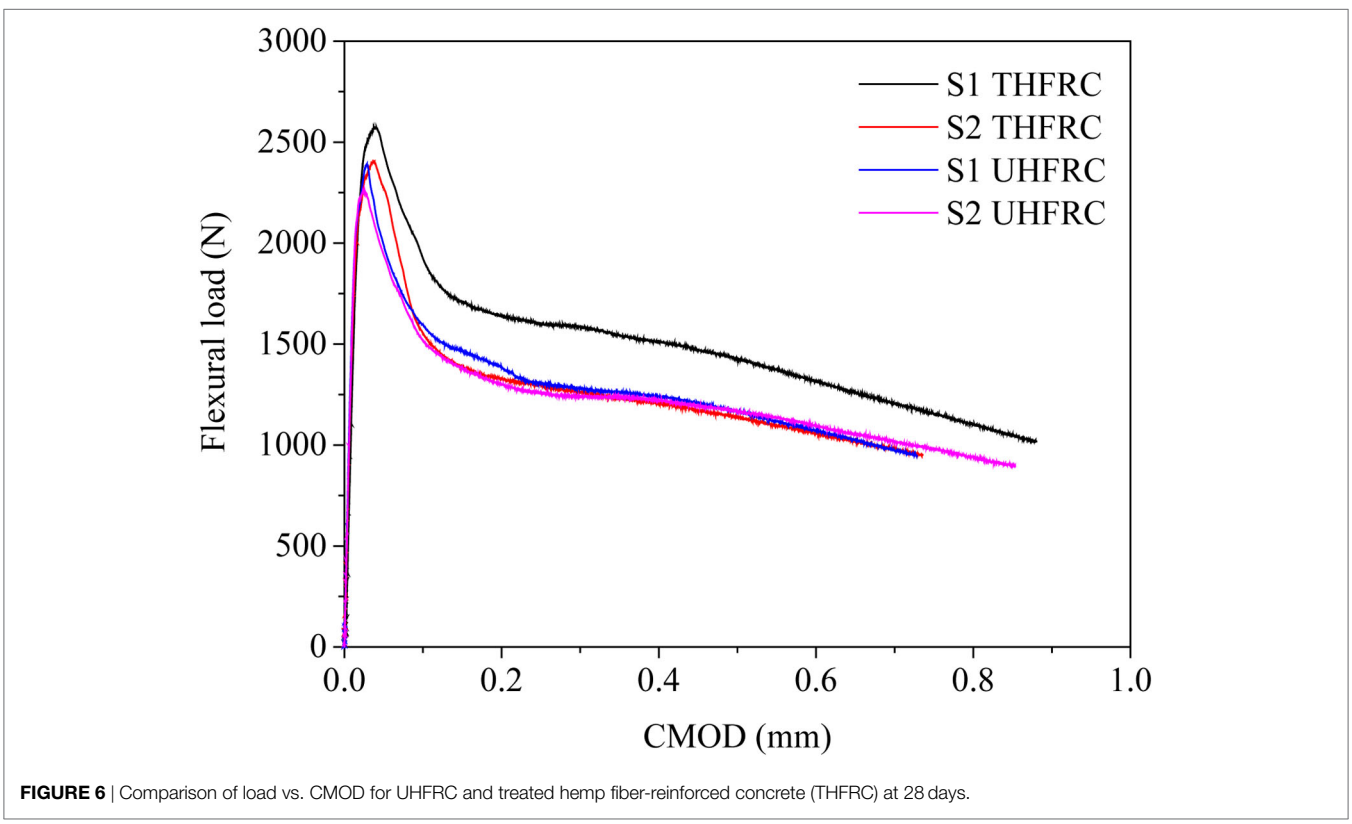

FIGURE 6 | Comparison of load vs. CMOD for UHFRC and treated hemp fiber-reinforced concrete (THFRC) at 28 days.

curves of UHFRC and THFRC; two samples were tested for UHFRC and THFRC represented by S1 and S2. The area under the flexural load vs. CMOD curve represents the total fracture energy, which remains fairly similar for both UHFRC and THFRC at 14 and 28 days. However, THFRC is seen to cover a slightly larger area indicating it has slightly greater fracture energy (Zhou et al., 2013). Additionally, the unloading curve is seen to be very similar for both the UHFRC and THFRC. However, THFRC is seen to display slightly higher ductility due to the increased extension of the curve.

The critical stress intensity factor (K^s_{IC}) essentially represents a material's fracture toughness as the ability to resist the propagation of a crack. The results from **Table 2** indicate that higher K^s_{IC} values were found for specimens that include treated hemp fiber, and at longer curing ages. At the ages of 14 and 28 days, THFRC has a K^s_{IC} value of 15.3 and 19.7% greater than UHFRC, respectively. This could be explained by the treated fibers increased surface roughness (shown previously in **Figure 3B**) that bind to the matrix more efficiently (Mwaikambo and Ansell, 2006), and the excess $Ca(OH)_2$ on the fibers being converted to additional CSH (as shown later in **Figure 8B**) (Rosenberg, 2010). In this case, THFRC would contain fewer imperfections such as voids or micro-cracks surrounding the fibers due to the additional CSH formation, meaning a greater amount of crack deflection occurs as the path of least resistance is around stronger particles that have formed through the increased pozzolanic reaction near the fibers (Li, 2011). Hence, the values for a_e and $CTOD_c$ are also larger for THFRC. In addition, the value for K^s_{IC} is seen to increase with the age of both THFRC and UHFRC, independently. This could be due to the interfacial bond that develops further with time, at early ages there is low hydration and as a result, the bond is less sufficient as the formation of CSH is low; however, this increases with time and the values are higher at greater ages (Chandra and Berntsson, 1997). With age, the concrete matrix and fibers form greater adhesion strength; and the matrix is able to keep fibers more tightly held, meaning they have a greater ability to resist propagation of cracking (Bentur and Mindess, 2007).

The critical strain energy release rate (G^s_{IC}) is the energy required for unit area crack extension at the start of unstable propagation. This must not be confused with the fracture energy (G_F) that is the average energy required for unit area crack propagation during the fracture process as a whole. There is a directly proportional relationship between the two, although in actual fact, G_F is larger than G^s_{IC}. The results presented in **Table 2** indicate that G^s_{IC} increases with the inclusion of treated fiber and age of specimens. These results display a very similar trend to that observed for K^s_{IC}, this is likely to be due to the fact that the peak load is directly related to K^s_{IC}, and this value in turn is used to calculate G^s_{IC}, hence, both follow the same trend. At the ages of 14 and 28 days, respectively, THFRC has a G^s_{IC} value in the region of 37.4 and 60.5%, greater than UHFRC. These increases could be explained by the ability of treated fibers to bridge cracks more efficiently and for a longer period of time. The rough surface allows them to anchor into the matrix very well as opposed to untreated fibers, and also the increased formation of CSH around the fibers avoids fiber pull-out from occurring as easily (Mwaikambo and Ansell, 2006; Liu et al., 2014). Furthermore, the value for G^s_{IC} is seen to increase again with the age, for both THFRC and UHFRC, independently.

The results for the modulus of elasticity (E) indicate the value decreases with the inclusion of treated fiber; however, it increases with age. The value for E is seen to decrease by 3.2 and 10.8%, at 14 and 28 days, respectively, for THFRC. This decrease could potentially be explained by the increase in strain capacity for treated fibers compared to untreated fibers, as also found by Mwaikambo and Ansell (2006). Consequently, the treated fibers undergo more appreciable deformation prior to rupture. This in turn means that THFRC behaves in a more ductile manner in comparison to UHFRC, hence, the lower values in E obtained. Additionally, the lower values of E for THFRC could be explained by the initial flexibility compliance (C_i), which is seen to directly affect the value for E, and is higher in both THFRC, at 14 and 28 days. This higher value is likely to be as a result of the improved ability of THFRC to sustain higher load and resist CMOD with increasing load, due to the improvement in load transfer process at the interface (Islam et al., 2010). On the other hand, the value for E is seen to increase with age for both THFRC and UHFRC, independently. At 14 days, THFRC and UHFRC have values of 17,015 and 17,584 MPa, respectively, while at 28 days, THFRC and UHFRC have values of 18,279 and 20,481 MPa, respectively. This could be explained by the decrease in ductility with age; the higher values indicate the specimens are stiffer which they are likely to be as these possess higher compressive strengths due to being of a mature age (this can be seen previously from the compressive results in **Figure 5**).

A quantity known as the brittleness number (Q) has also been introduced by Jenq and Shah (1985) in the TPFM. This parameter combines E, $CTOD_c$, and K^s_{IC} to dictate the brittleness of concrete. The value for Q, relative to UHFRC, is seen to increase for THFRC by 4.7 and 11.0%, at 14 and 28 days, respectively. This indicates THFRC is less brittle than UHFRC, as reduced values for Q indicate more brittle material behavior (Jenq and Shah, 1985). This is likely to be due to THFRC having enhanced ductility and also the higher values for $CTOD_c$ obtained as a result of improved crack bridging/deflection. The potential increase in surface area of treated fibers also means a greater amount of stress can be transferred, meaning THFRC can sustain higher stress before pull-out (Islam et al., 2010). Furthermore, the value for Q is seen to increase with age for both THFRC and UHFRC, independently. At 14 days, THFRC and UHFRC have values of 88.00 and 84.1 mm, respectively, while at 28 days, THFRC and UHFRC have values of 108 and 97.4 mm, respectively. Additionally, this again could be explained by $CTOD_c$, and the increase in this quantity with age.

In summary, it can be said the results indicate that THFRC has greater fracture toughness in relation to UHFRC. THFRC displays greater values for G^s_{IC} and K^s_{IC}, as well as better ductility properties (reduced E), and reduced brittleness (increased Q). This is likely to be due to the ability of THFRC to transfer stress across a larger zone to prevent propagation of cracks, and also the ability to bridge cracks more effectively. The rough treated fiber surface and residue also play a great role in dictating the properties that have been found. Additionally, it is evident that with age the fracture toughness of THFRC increases further as

the bond between the matrix and fiber advances further due to CSH formation. Moreover, the slight variation in results between specimens is likely to be the result of the heterogeneous nature of FRC, due to factors such as the fiber orientation, dispersion, and void content.

SEM Analysis of Cementitious Composite after Testing

Both UHFRC and THFRC displayed a combination of fiber pull-out and fiber rupture that is most likely due to the lack of homogeneity in HFRC. For example, there is likely to be variations in tensile strength, orientation, and other properties that vary between individual fibers that are set into the matrix. Overall, UHFRC displayed less sufficient bonding between the fiber and concrete matrix, as generally, more fibers were seen to be pulled out as shown in **Figure 7A**. This is most likely to be a result of the smooth fiber surface as observed in the initial SEM analysis prior to testing. A smoother surface would indicate less friction between the two bonding surfaces resulting in fibers requiring a lower load to be pulled out (Islam et al., 2010). The latter point is supported by the results of the fracture, which indicated UHFRC failed at a lower load compared to THFRC. In comparison, THFRC displayed more sufficient bonding between the fiber and concrete matrix, as generally, more fibers were seen to be intact as shown in **Figure 7B**. This is likely to be the result of the rough fiber surface as observed in the initial SEM analysis prior to testing. The interfacial adhesion strength is likely to get stronger for treated fibers, and consequently, improves the load transfer process at the interface (Islam et al., 2010).

When exposed fibers set in the concrete matrix were studied, the untreated fiber surface appeared smooth with hardly any concrete products attached to it as presented in **Figure 8A**. It is clear to see that composite failure between the fiber and matrix tended to occur closer to the fiber surface in UHFRC, indicating a weakness where the two surfaces meet. This demonstrates the poor adhesion capability of untreated fiber, as the concrete matrix has an insufficient surface to attach itself to. In comparison, the treated fiber surface appeared rough with a significant amount of debris attached to it as presented in **Figure 8B**. It is clear to see that composite failure between the fiber and concrete matrix tended to occur slightly further from the fiber surface in THFRC, indicating less weakness between where the two surfaces meet and in fact, a weakness in the concrete matrix. This demonstrates the excellent adhesion capability of treated fibers, as the concrete products have a sufficiently rigid surface to anchor/attach onto.

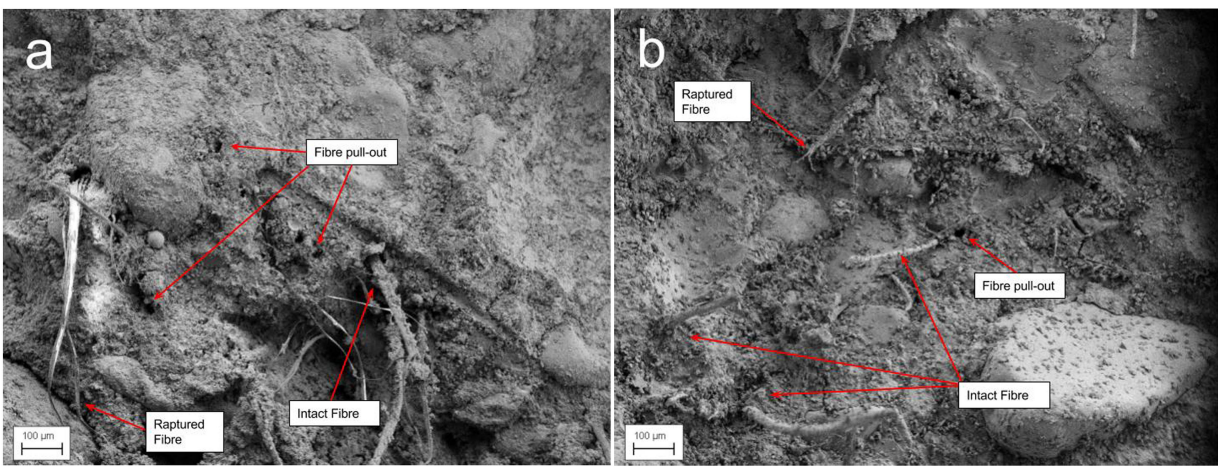

FIGURE 7 | Fiber pull-out and fiber rupture observed at ×200 magnification: **(A)** UHFRC and **(B)** treated hemp fiber-reinforced concrete (THFRC).

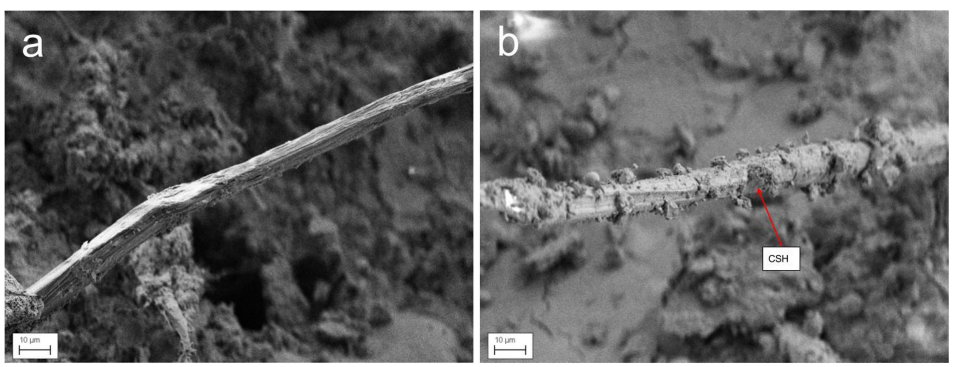

FIGURE 8 | Exposed fiber surface after composite failure at ×2,000 magnification: **(A)** untreated fiber and **(B)** treated fiber.

CONCLUSION

The main aim of this study was to promote the use of natural hemp fibers to reinforce cementitious construction materials. THFRC has been able to provide significant advantages over UHFRC, allowing it to address the current issues faced with using untreated fiber. With regard to the objectives of this study, the following conclusions can be made about the inclusion of treated hemp fibers in concrete:

- Treatment of hemp fibers using alkali $Ca(OH)_2$ solution led increased surface roughness that improves the interfacial bond and adhesion and to an increased pozzolanic reaction surrounding the fibers that resulted in increased production of CSH.
- Treated hemp fibers provide increased early compressive strength of THFRC, with the largest increase present between 7 and 14 days, compared to UHFRC that was between 14 and 28 days. In addition, THFRC is recorded to be not only less brittle but also more ductile. This means the composite is more durable and more resistant to long-term cracking.
- Increase in overall fracture toughness of THFRC through greater values for the critical stress intensity factor (K^s_{IC}) and critical strain energy release rate (G^s_{IC}) indicates the composite can absorb larger amounts of energy prior to failure. The treated fibers also provide a greater amount of post-fracture stress transfer ability.

AUTHOR CONTRIBUTIONS

XZ is the corresponding author and supervised the research done by two students as co-author. HS is a master student who did the experimental work, analyzed the data, and drafted the paper. GK is a PhD student and contributed to the research work and writing.

FUNDING

Partial financial support from the European Commission Horizon 2020's MARIE Skłodowska-CURIE Research and Innovation Staff Exchange scheme through the grant agreement 645696 (i.e., REMINE project) is greatly acknowledged.

REFERENCES

Awwad, E., Mabsout, M., Hamad, B., Farran, M. T., and Khatib, H. (2012). Studies on fiber-reinforced concrete using industrial hemp fibers. *Constr. Build. Mater.* 35, 710–717. doi:10.1016/j.conbuildmat.2012.04.119

Bentur, A., and Mindess, S. (2007). *Fibre Reinforced Cementitious Composite*, 2nd Edn. London: Taylor and Francis.

Bledzki, A. K., Sperber, V. E., and Faruk, O. (2002). "Survey of natural fibre composites," in *Natural and Wood Fibre Reinforcement in Polymers*, ed. S. Humphreys (Shropshire: Rapra Technology LTD), 3.

British Standards Institute. (2009a). *BS EN 12390-3-2009 Testing Hardened Concrete – Part 3: Compressive Strength of Test Specimens*. London, UK: BSI.

British Standards Institute. (2009b). *BS EN 12390-6-2009 Testing hardened Concrete – Part 6: Tensile Splitting Strength of Tests Specimens*. London, UK: BSI.

Chandra, S., and Berntsson, L. (1997). "Use of silica fume in concrete," in *Waste Materials Used in Concrete Manufacturing*, ed. S. Chandra (New Jersey: Noyes Publications), 554–614.

Concerted Action Energy Performance of Buildings. (2010). *Directive 2010/31/EU of the European Parliament and of the Council of 19 May 2010 on the Energy Performance of Buildings*. 13–35. Available at: http://eur-lex.europa.eu/LexUriServ/LexUriServ.do?uri=OJ:L:2010:153:0013:0035:EN:PDF

Denneman, E., Kearsley, E. P., and Visser, A. T. (2011). Splitting tensile test for fibre reinforced concrete. *Mater. Struct.* 44, 1441–1449. doi:10.1617/s11527-011-9709-x

GOV. (2011). *The Carbon Plan: Delivering Our Low Carbon Future*. Available at: https://www.gov.uk/government/uploads/system/uploads/attachment_data/file/47613/3702-the-carbon-plan-delivering-our-low-carbon-future.pdf

Holister, G. S., and Thomas, C. (1966). *Fibre Reinforced Materials*. London: Elsevier Publishing Co. Ltd.

Islam, M. S., Pickering, K. L., and Foreman, N. J. (2010). Influence of alkali treatment on the interfacial and physico-mechanical properties of industrial hemp fibre reinforced polylactic acid composites. *Compos. Part A. Appl. Sci. Manuf.* 41, 596–603. doi:10.1016/j.compositesa.2010.01.006

Jenq, Y., and Shah, S. (1985). Two-parameter fracture model for concrete. *J. Eng. Mech.* 111, 1227–1241. doi:10.1061/(ASCE)0733-9399(1985)111:10(1227)

Li, Z. (2011). "Concrete fracture mechanics," in *Advanced Concrete Technology*, eds G. C. K. Chau, B. Xu, and J. Shen (New Jersey: John Wiley and Sons), 326–379.

Liu, J., Qiu, Q., Xing, F., and Pan, D. (2014). Permeation properties and pore structure of surface layer of fly ash concrete. *Materials* 7, 4282–4296. doi:10.3390/ma7064282

Mehta, P. K., and Monteiro, P. J. M. (2006). "Fibre-reinforced concrete," in *Concrete: Microstructure, Properties, and Materials*, 3rd Edn (New York: McGraw-Hill), 502–522.

Merta, I., and Tschegg, E. K. (2013). Fracture energy of natural fibre reinforced concrete. *Constr. Build. Mater.* 40, 991–997. doi:10.1016/j.conbuildmat.2012.11.060

Morgan, J. (2014). *Hemp Fibres 'Better Than Graphene'*. BBC News: Science and Environment. Available at: http://www.bbc.co.uk/news/science-environment-28770876

Mwaikambo, L. Y., and Ansell, M. P. (2006). Mechanical properties of alkali treated plant fibres and their potential as reinforcement materials. I. hemp fibres. *J. Sci. Mater.* 41, 2483–2496. doi:10.1007/s10853-006-5098-x

Ray, D. (2015). "State-of-the-art applications of natural fiber composites in the industry," in *Natural Fiber Composites*, 1st Edn, ed. R. D. S. G. Campilho (Boca Raton, FL: CRC Press), 319–340.

Rijswijk, K. V., Brouwer, W. D., and Beukers, A. (2003). *Application of Natural Fibre Composites in the Development of Rural Societies*. Structures and Materials Laboratory Faculty of Aerospace Engineering Delft University of Technology. Available at: http://www.fao.org/docrep/007/ad416e/ad416e00.htm

RILEM Draft Recommendations TC 50-FMC. (1985). Determination of the fracture energy of mortar and concrete by means of three-point bend test on notched beams. *Mater. Struct.* 18, 287–290. doi:10.1007/BF02472918

RILEM Draft Recommendations TC 89-FMT. (1990). Determination of fracture parameters (K^s_{IC} and $CTOD_c$) of plain concrete using three-point bend test. *Mater. Struct.* 23, 457–460.

Rosenberg, A. (2010). *Using Fly Ash in Concrete*. National precast concrete association, Precast Magazine. Available at: http://precast.org/2010/05/using-fly-ash-in-concrete/

Sedan, D., Pagnoux, C., Smith, A., and Chotard, T. (2007). Mechanical properties of hemp fibre reinforced cement: influence of the fibre/matrix interaction. *J. Eur. Ceram. Soc.* 28, 183–192. doi:10.1016/j.jeurceramsoc.2007.05.019

Stevulova, N., Cigasova, J., Estokova, A., Terpakova, E., Geffert, A., Kacik, F., et al. (2014). Properties characterization of chemically modified hemp hurds. *Materials* 7, 8131–8150. doi:10.3390/ma7128131

Thomas, M. (2007). *Concrete-Optimizing the Use of Fly Ash in Concrete*. Illinois: Portland Cement Association, 1–24.

Xu, S., and Reinhardt, H. W. (1998). Crack extension resistance and fracture properties of quasi-brittle softening materials like concrete based on the complete process of fracture. *Int. J. Fract.* 92, 71–99. doi:10.1023/A:1007553012684

Xu, S., and Reinhardt, H. W. (2000). A simplified method for determining double-*K* fracture parameters for three-point bending tests. *Int. J. Fract.* 104, 181–209. doi:10.1023/A:1007676716549

Zhou, X., Ghaffar, S. H., Dong, W., Oladiran, O., and Fan, M. (2013). Fracture and impact properties of short discrete jute fibre-reinforced cementitious composites. *Mater. Des.* 49, 35–47. doi:10.1016/j.matdes.2013.01.029

Conflict of Interest Statement: The authors declare that the research was conducted in the absence of any commercial or financial relationships that could be construed as a potential conflict of interest.